

Microstrip Feed Slotted Ground Antenna with Parasitic Element for UWB Applications

Girish Awadhwal and Ali Bostani

Abstract A novel method to develop an Ultra-Wide Band (UWB) antenna is proposed in which a defected ground structure technique is employed. The proposed design is excited via a microstrip feed line which is optimized for the best impedance matching performance. The slotted ground is to enhance the UWB performance. The design parameters of the antenna have been optimized using high frequency finite element-based simulation software for the best gain, bandwidth and efficiency performance. The final design successfully meets the requirements of the UWB and even exceeds them, having a bandwidth of 2.55 to 10.85 GHz. The design parameters and the simulation results are reported in this paper and include the radiation pattern at different frequencies within the operating band.

1 Introduction

Higher data transmission rates and expanding high speed communication involving a lot of multimedia data transfer require the trajectory of technological advancement to take a detour along the path of bandwidth enhancement. The large amount of attention that has been devoted to the design and expansion of ultra-wide band (UWB) antennas was a response from scientists in the fields of RF and microwave studies to this demand from the market. These days, UWB antennas have several applications in radar communication such as RF identification devices, high-tech sensor networks, positioning and tracking systems, and in many other wireless communication fields.

G. Awadhwal

Department of Electronics and Communication Engineering Department,
University Institute of Technology RGPV, Bhopal, India
e-mail: Girish.awadhwal.ece10@itbhu.ac.in

A. Bostani (✉)

Electrical Engineering Department, American University of the Middle East,
Egaila, Kuwait
e-mail: ali.bostani@aum.edu.kw

To meet the needs of modern compact portable devices, the best choice for the design of UWB antennas would be a low profile and lightweight option such as printed antennas. This is the reason that we see all kinds of microstrip designs of UWB antenna reported in publications [1–3]. In 2002, the federal communication commission (FCC) allocated a frequency band from 3.1 to 10.6 GHz for commercial applications of UWB [1]. Since then, several designs for UWB antennas [4–6] have been proposed using several different shapes such as square [1], circular [7], pentagonal [2], hexagonal [4], elliptical [5], ring [6] and trapezoidal [8]. There are also various configurations and design techniques, which includes monopoles [1, 2, 5], dipoles and slot antennas [4] and various feeding techniques such as micro-strip [1, 5–7], co-planar-waveguide (CPW) [7]. Lin and Wong [4] and Morioka et al. [8] also used coaxial [9] all those mentioned were successfully employed in UWB applications.

Amongst all the mentioned designs and techniques, printed monopole antennas have received much more attention due to their wideband characteristic, Omni-directional radiation patterns, high radiation efficiency, and compact size [8, 10]. Recent technological advances in the size reduction of electronic circuits have changed wireless communications and sensor network design specifications. In particular, they have exposed the need for electrically small antennas that are efficient and have significant bandwidths. The standard electrically small antenna designs are known to be inefficient due to their large reactance and low resistance, which leads to the poor match to a given source. However, to compensate the impedance mismatch and additional bandwidth, researchers have already introduced the concept of defected ground structure (DGS), defected micro-strip structure (DMS) and other types of defect either in the feed line or in the body of the antenna itself.

On the other hand, the finite element method has been successfully employed to analyze and optimize the design of UWB antennas because of its accuracy and ability to handle the unconventional geometries [11, 12].

In this paper, a defected ground antenna is proposed which is designed based on the DGS concept and optimized for the best performance in terms of impedance matching within the UWB band and the radiation pattern and the gain using high frequency full wave finite element simulation software.

Details of the design concept of the antenna and simulation results are described in Sects. 2 and 3 respectively, as discussed in this section, and the conclusions are described in Sect. 4.

2 Antenna Design

Figure 1 shows the configuration of the proposed wideband antenna which consists of a slotted ground feed by micro-strip line. The proposed antenna, which has compact dimensions of $28 \times 32 \text{ mm}^2$ is constructed on an FR4 substrate with a thickness of 1.6 mm and relative dielectric constant of 4.4. The width of the

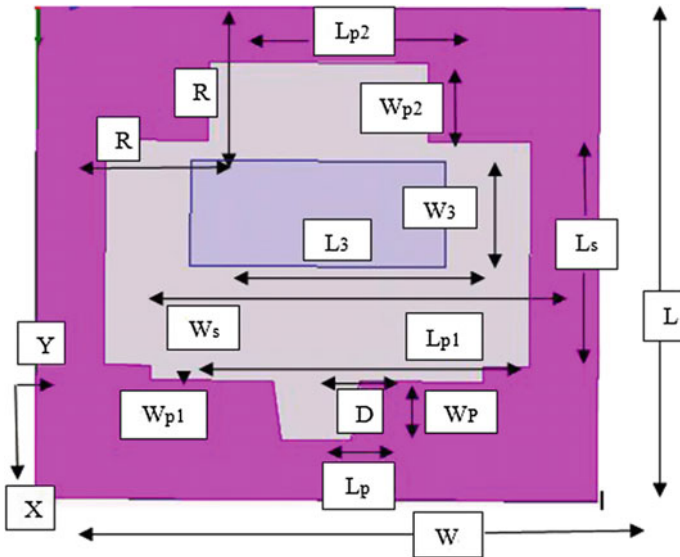


Fig. 1 Top view of the proposed microstrip feed slotted ground antenna

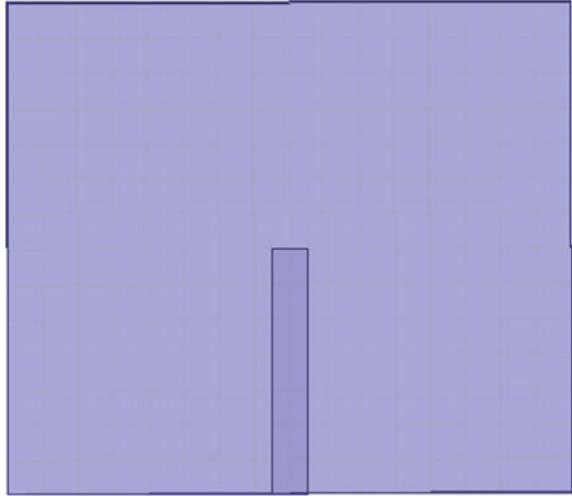
micro-strip feed line is fixed at 2 mm and has a length of 14 mm. The downside of ground slot has an upper side length $D = 5$ mm and a lower side length of $L_p = 4$ mm. The direction of the Z axis is out of the plane. To achieve the maximum impedance bandwidth all the proposed antenna design parameters are optimized by HFSS software. The optimal dimensions of the designed antenna are as follows: $W = 32$ mm, $L = 28$ mm, $L_p = 4$ mm, $W_p = 3.5$ mm, $R = 8.75$ mm, $D = 5$ mm, $W_f = 2$ mm, $L_f = 14$ mm, $W_s = 24.25$ mm, $L_s = 12.8$ mm, $W_{p1} = .875$ mm, $L_{p1} = 19$ mm, $W_{p2} = 4.5$ mm, $L_{p2} = 12.5$ mm, $W_3 = 6$ mm, $L_3 = 14.5$ mm.

The antenna was modeled on a 3D cad and was simulated using high frequency full wave finite element based simulation software. The tetrahedral elements were chosen to make sure that there are no singularities within the entire geometry and the mesh is fine enough to ensure the accuracy of the obtained results. Several passes of the finite element solver confirmed that the designed antenna satisfies all the requirements in the UWB frequency band and show that the impedance matching bandwidth of the antenna can cover a range of 2.58 to 10.74 GHz.

3 Results and Discussions

A parametric study of the proposed antenna was carried out in order to achieve UWB operation. The slots on the ground plane are optimized to make sure that the antenna meets the UWB requirement. To reduce the complexity of the design, some antenna

Fig. 2 Bottom view of the proposed microstrip feed slotted ground antenna



parameters were selected to be fixed as shown in Fig. 1. In this section the effects of the parameters W_f , L_f , W_s , $Wp1$, $Lp1$, $Wp2$, $Lp2$, $W3$, $L3$ on the antenna's performance are reported in detail (Fig. 2).

3.1 Parametric Study of the Effects of Variation of the Feed Line Width (W_f)

Figure 3 illustrates the return loss (S_{11}) plot of the UWB antenna for different values of W_f . It can be seen that the resonant frequencies and operating bandwidth depend on this parameter. The optimized value of W_f was found to be 2.2 mm.

3.2 Parametric Study of the Effects of Variation of the Feed Line Length (L_f)

Figure 4 illustrates the return loss (S_{11}) plot of the UWB antenna for different values of feed line length L_f . It can be seen that the upper cutoff frequency and operating bandwidth depend on this parameter. The optimized value of W_f was found to be 14 mm.

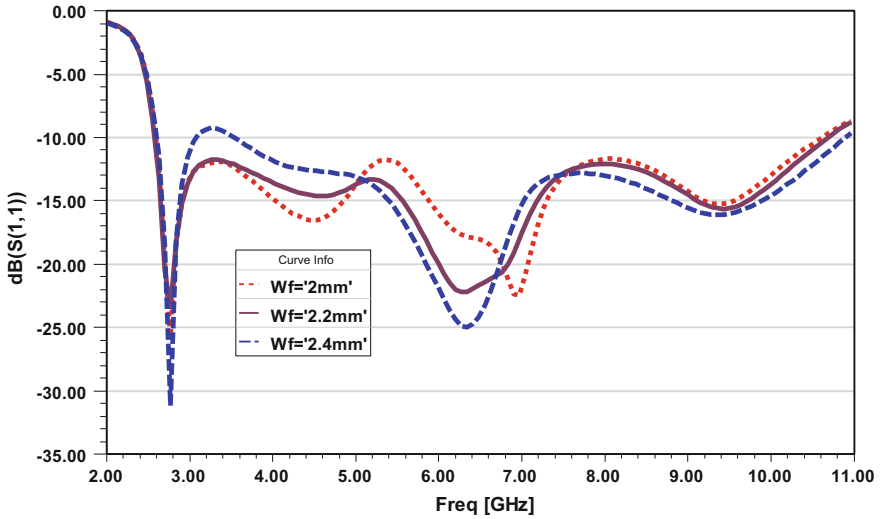


Fig. 3 Simulated return loss against frequency for the proposed antenna with varying feed line width W_f ; other parameters are same as in Fig. 2

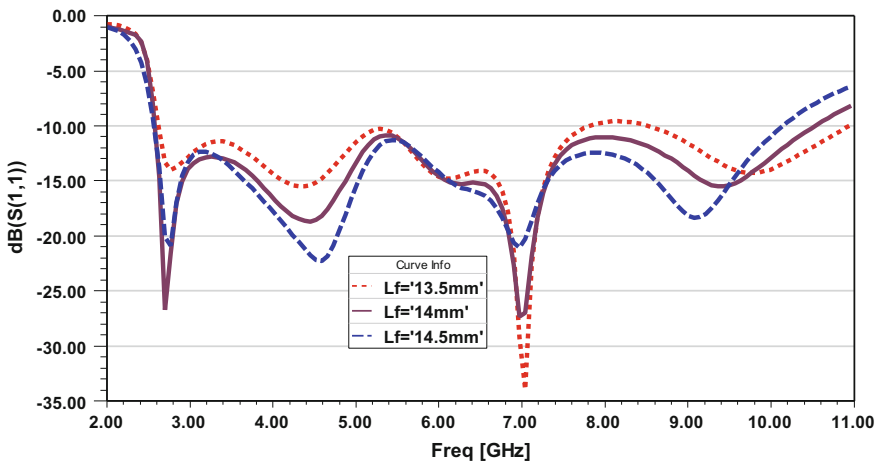


Fig. 4 Simulated return loss against frequency for the proposed antenna with varying feed line length L_f ; other parameters are same as in Fig. 2

3.3 Parametric Study of the Effects of Variation of the Ground Slot Parameter W_s

Figure 5 illustrates the return loss (S_{11}) plot of the UWB antenna for different values of slot parameter W_s . It can be seen that the upper cutoff frequency,

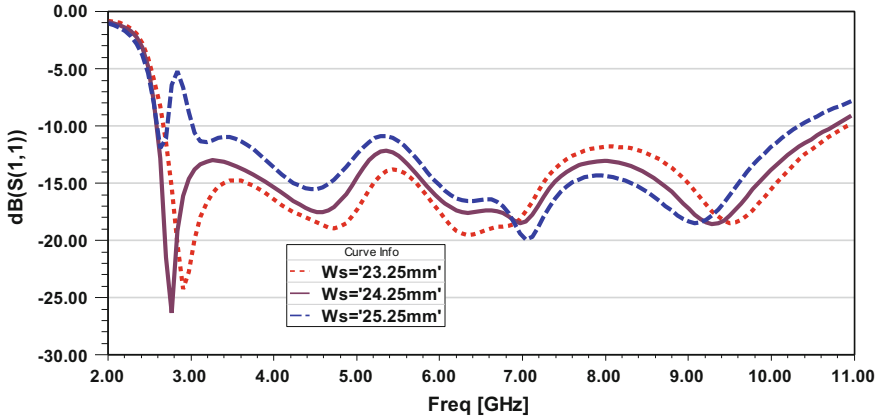


Fig. 5 Simulated return loss against frequency for the proposed antenna with varying ground slot parameter W_s ; other parameters are same as in Fig. 1

resonance frequency and operating bandwidth depend on this parameter. The optimized value of W_s was found to be 24.25 mm.

3.4 Parametric Study of the Effects of Variation of the Ground Slot Parameter W_{p1}

Figure 6 illustrates the return loss (S_{11}) plot of the UWB antenna for different values of parameter W_{p1} . It can be seen that the resonance frequency, upper cutoff

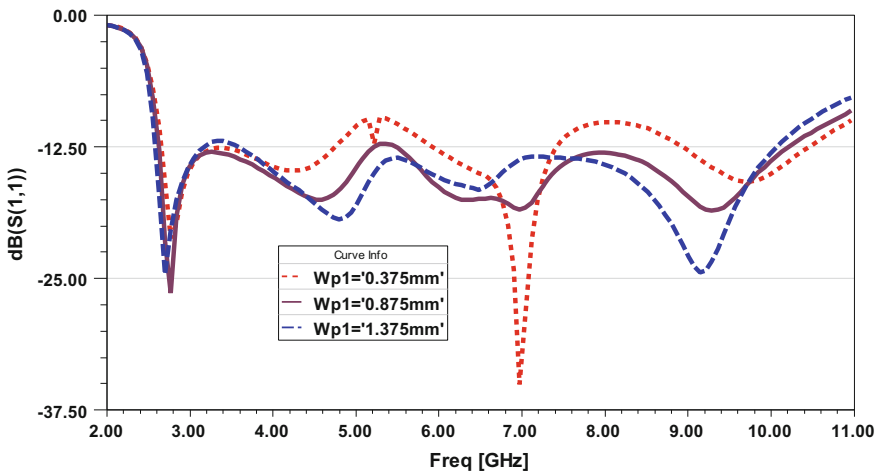


Fig. 6 Simulated return loss against frequency for the proposed antenna with varying ground slot parameter W_{p1} ; other parameters are same as in Fig. 1

Frequency and operating bandwidth depend on this parameter. The optimized value of $Wp1$ was found to be 0.875 mm.

3.5 Parametric Study of the Effects of Variation of the Ground Slot Parameter $Lp1$

Figure 7 illustrates the return loss (S_{11}) plot of the UWB antenna for different values of parameter $Lp1$. It can be seen that the upper cutoff frequency depends on this parameter. The optimized value of parameter $Lp1$ was found to be 19 mm.

3.6 Parametric Study of the Effects of Variation of the Ground Slot Parameter $Wp2$

Figure 8 illustrates the return loss (S_{11}) plot of the UWB antenna for different values of parameter $Wp2$. It can be seen that the resonance frequency depends on this parameter. The optimized value of parameter $Wp2$ was found to be 4.5 mm.

3.7 Parametric Study of the Effects of Variation of the Ground Slot Parameter $Lp2$

Figure 9 illustrates the return loss (S_{11}) plot of the UWB antenna for different values of parameter $Lp2$. It can be seen that the resonant frequency depends on this parameter. The optimized value of parameter $Lp2$ was found to be 6.25 mm.

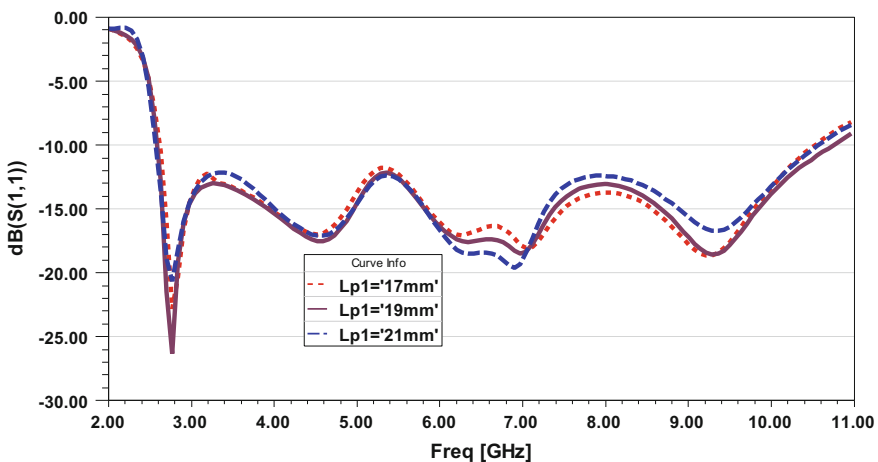


Fig. 7 Simulated return loss against frequency for the proposed antenna with varying slot parameter $Lp1$; other parameters are same as in Fig. 1

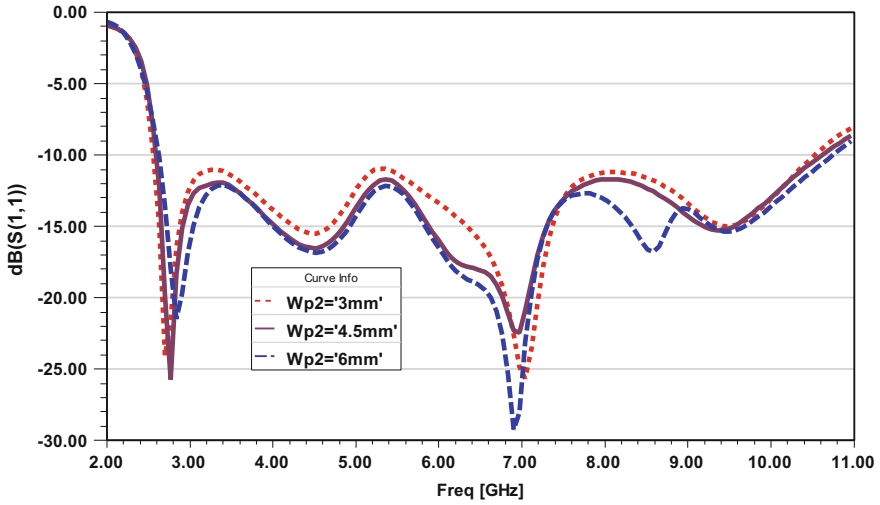


Fig. 8 Simulated return loss against frequency for the proposed antenna with varying ground slot parameter Wp2; other parameters are same as in Fig. 1

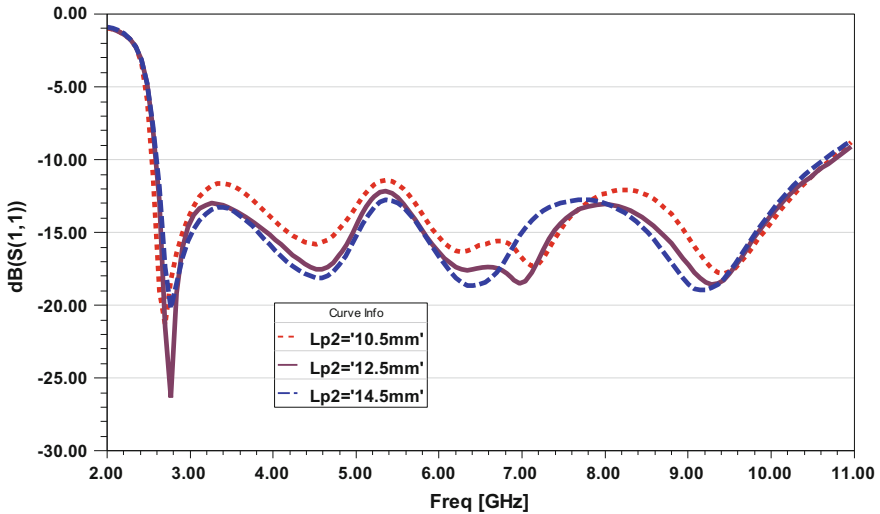


Fig. 9 Simulated return loss against frequency for the proposed antenna with varying slot parameter Lp2; other parameters are same as in Fig. 1

3.8 Parametric Study of the Effects of Variation of the Parasitic Element Parameter W_3

Figure 10 illustrates the return loss (S_{11}) plot of the UWB antenna for different values of parameter W_3 . It can be observed that the lower cutoff frequency, upper cutoff frequency and resonant frequency depend on this parameter. The optimized value of parameter W_3 was found to be 6 mm.

3.9 Parametric Study of the Effects of Variation of the Parasitic Element Parameter L_3

Figure 11 illustrates the return loss (S_{11}) plot of the UWB antenna for different values of parameter L_3 . It can be seen that the resonance frequency depends on this parameter. The optimized value of parameter W_3 was found to be 14.5 mm.

3.10 The Optimized Structure

Figure 12 illustrates the return loss plot of the simulated optimized structure of the micro-strip feed slotted ground antenna which covers the UWB. Figure 13 illustrates the VSWR (1) plot of the simulated optimized structure of the micro-strip feed slotted ground antenna, which is less than 2 above the UWB.

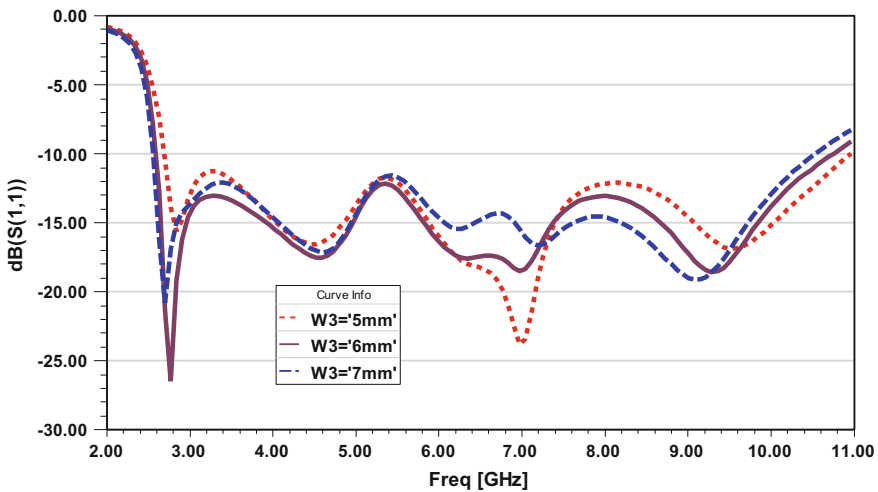


Fig. 10 Simulated return loss against frequency for the proposed antenna with varying parameter W_3 ; other parameters are same as in Fig. 1

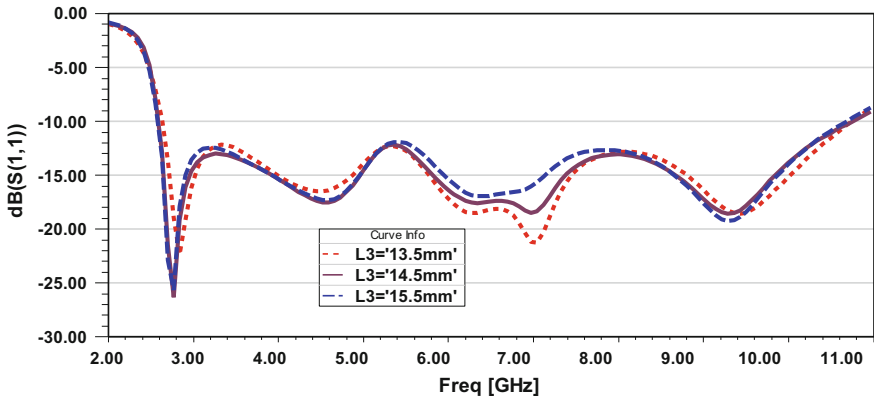


Fig. 11 Simulated return loss against frequency for the proposed antenna with varying parameter W_3 ; other parameters are same as in Fig. 1

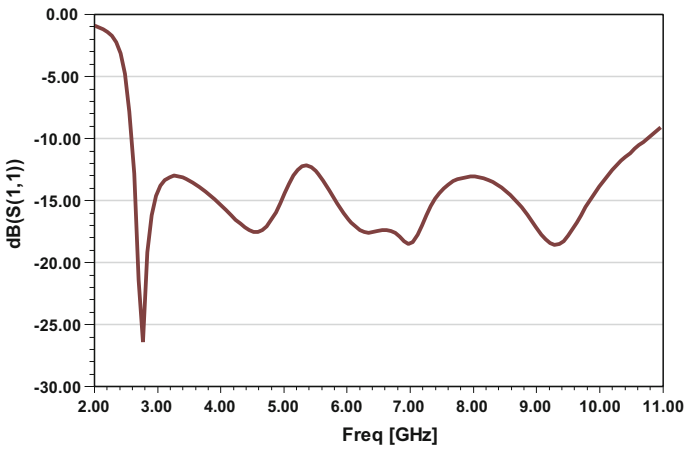


Fig. 12 Simulated return loss against frequency for the proposed optimized micro-strip feed slotted ground antenna

The radiation characteristics were also investigated. Figures 13, 14, 15, 16, 17, 18, 19 present the far field 10 dB normalized radiation patterns of the E plane and the H plane for the designed antenna at 2.7, 3.5, 4.31, 5.57, 6.55, 7.25, 9.7 and 10.54 GHz. The radiation pattern is directive for both E_plane and H_plane withing the whole frequency band. (Figs 20, 21, 22, 23).

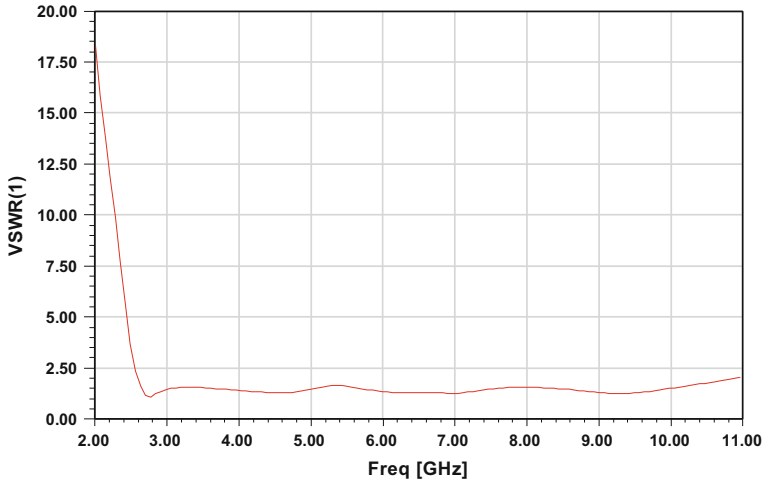


Fig. 13 Simulated VSWR against frequency for the proposed optimized micro-strip feed slotted ground antenna

Fig. 14 Radiation pattern for 2.7 GHz. Solid line shows E Plane ($\phi = 0^\circ$), Long dash shows H Plane ($\phi = 90^\circ$)

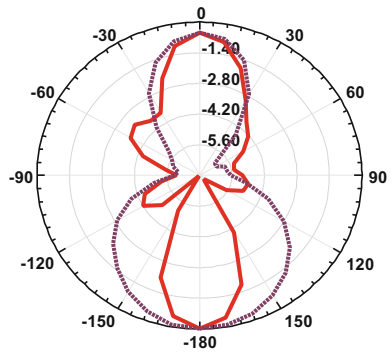


Fig. 15 Radiation pattern for 3.4 GHz. Solid line shows E Plane ($\phi = 0^\circ$), Long dash shows H Plane ($\phi = 90^\circ$)

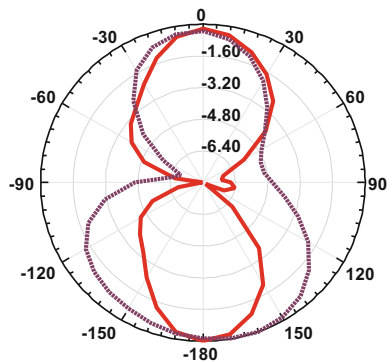


Fig. 16 Radiation pattern for 4.31 GHz. Solid line shows E Plane ($\phi = 0^\circ$), Long dash show H Plane ($\phi = 90^\circ$)

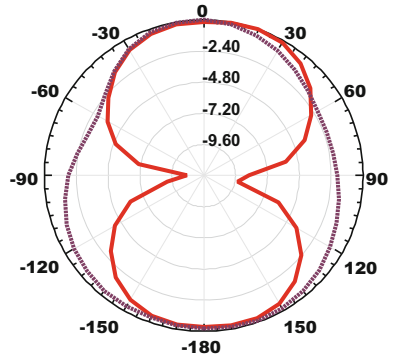


Fig. 17 Radiation pattern for 5.57 GHz. Solid line show E Plane ($\phi = 0^\circ$), Long dash shows H Plane ($\phi = 90^\circ$)

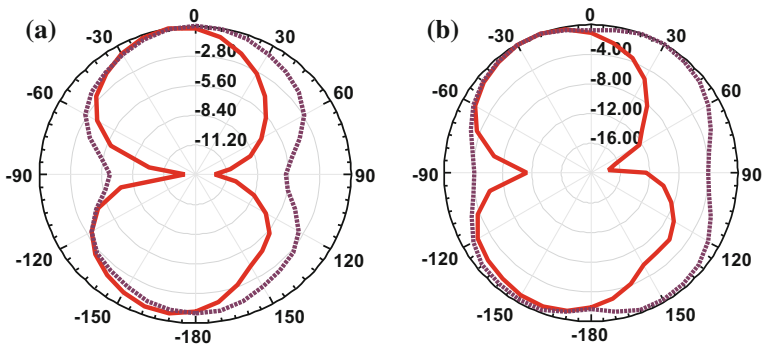
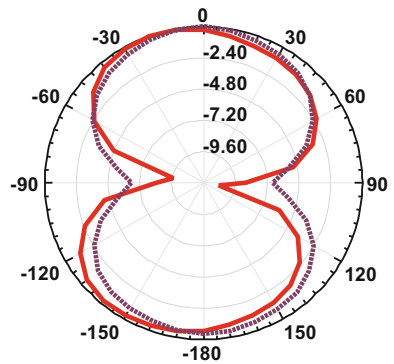


Fig. 18 **a** Radiation pattern for 6.55 GHz. Solid line shows E Plane ($\phi = 0^\circ$), Long dash shows H Plane ($\phi = 90^\circ$). **b** Radiation pattern for 7.25 GHz. Solid line shows E Plane ($\phi = 0^\circ$), Long dash shows H Plane ($\phi = 90^\circ$)

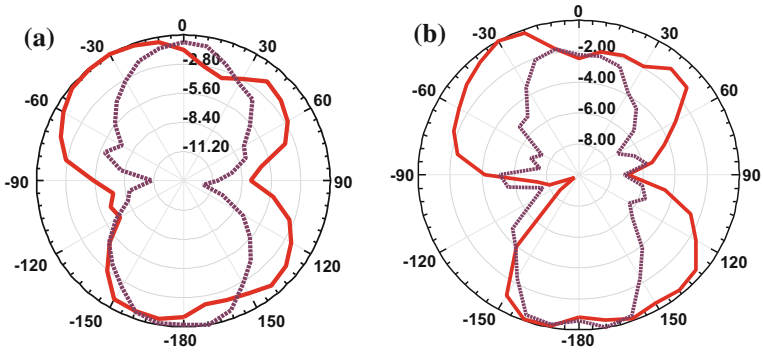


Fig. 19 a Radiation pattern for 9.7 GHz. Solid line shows E Plane ($\phi = 0^\circ$), Long dash shows H Plane ($\phi = 90^\circ$). b Radiation pattern for 10.54 GHz. Solid line shows E Plane ($\phi = 0^\circ$), Long dash shows H Plane ($\phi = 90^\circ$)

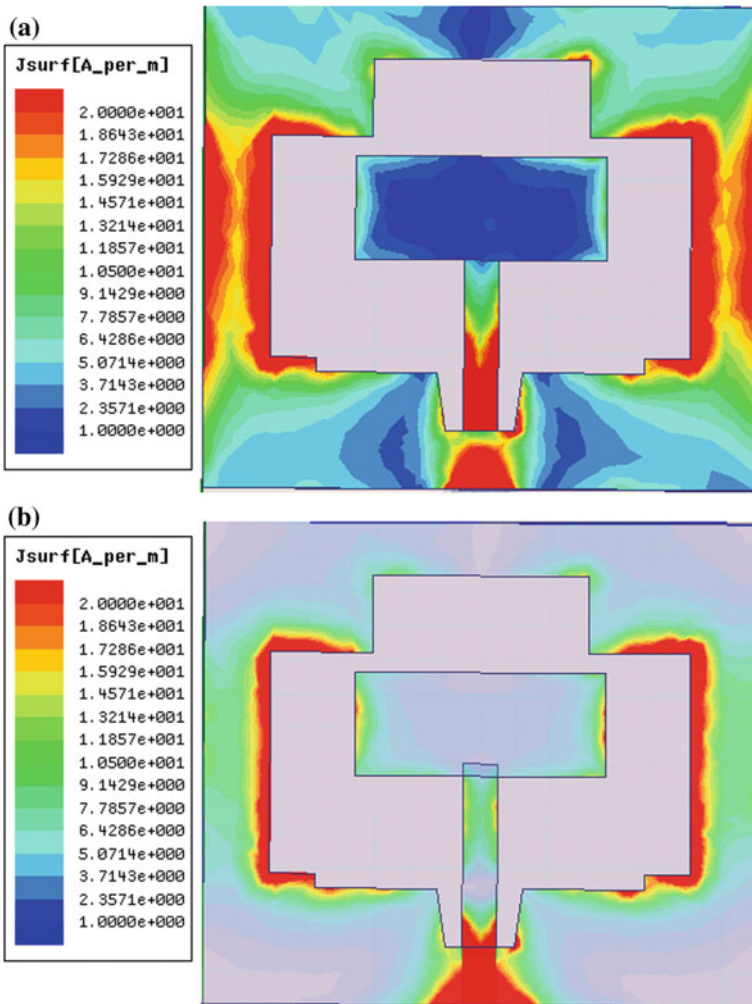


Fig. 20 a 3.3 GHz. b 4.3 GHz

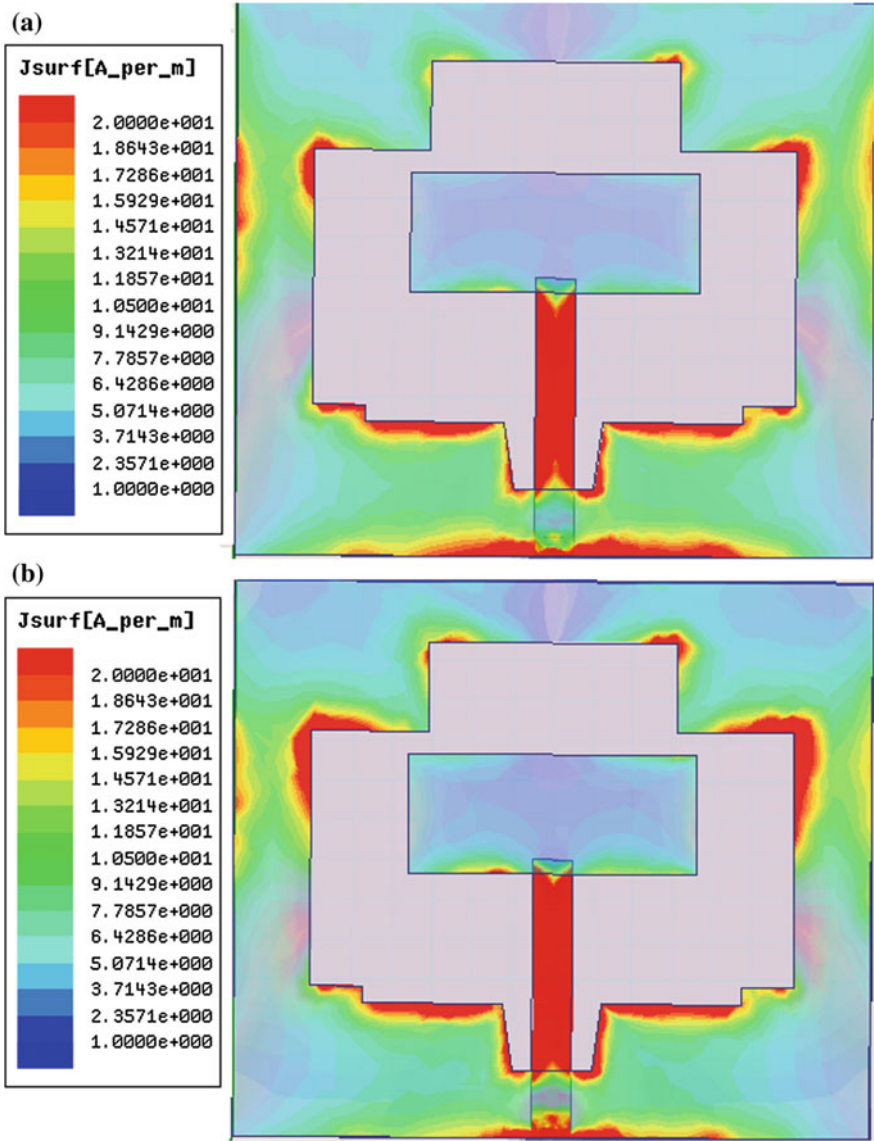


Fig. 21 a 5.1 GHz. b 6.06 GHz

Figure 30 shows the current density at different frequencies on the micro-strip feed line, parasitic element and slotted ground. At 3.3 GHz and 10.4 GHz the current density is concentrated on the slotted ground, parasitic element and feed line but for the remaining frequency current density is high on the feed-line and slotted ground compared to the parasitic element (Figs. 24, 25, 26, 27, 28, 29, 30).

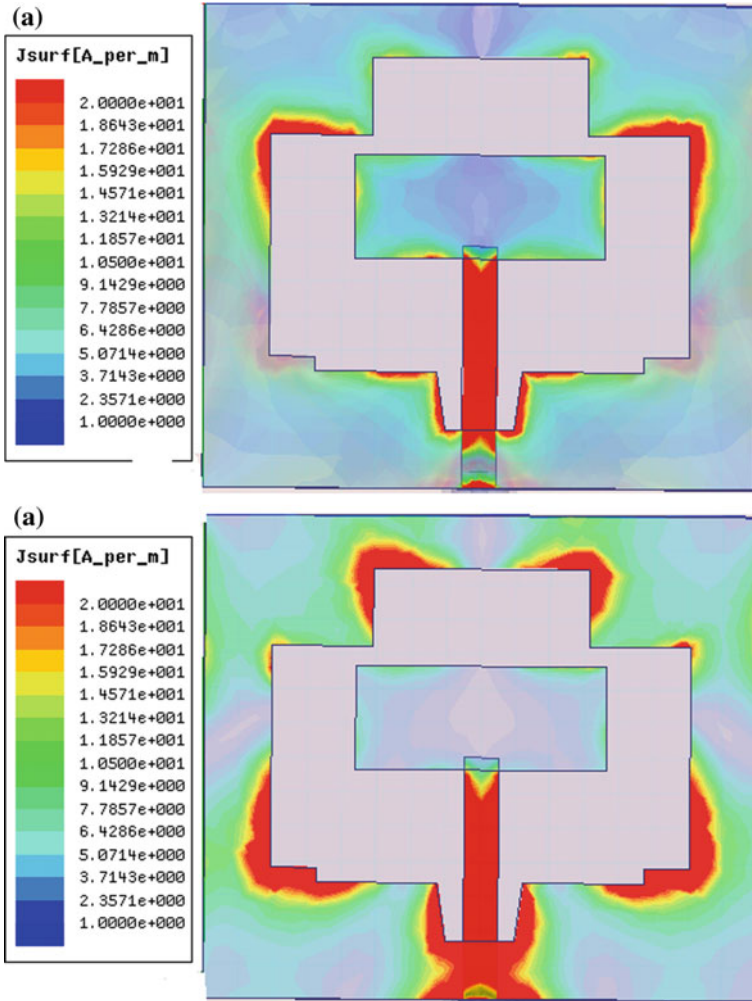


Fig. 22 a 7 GHz. b 8 GHz

Figures 24, 25, 26, 27, 28, 29, 30 show the total gain for different frequencies. At frequency 3.05 GHz, the total gain is maximum for $\theta = 180^\circ$. At frequency 7, 4.1 and 10.4 GHz the total gain is maximum for $\theta = 0^\circ$ and $\theta = 180^\circ$. At frequency 5.5 GHz total gain is maximum for all values of θ .

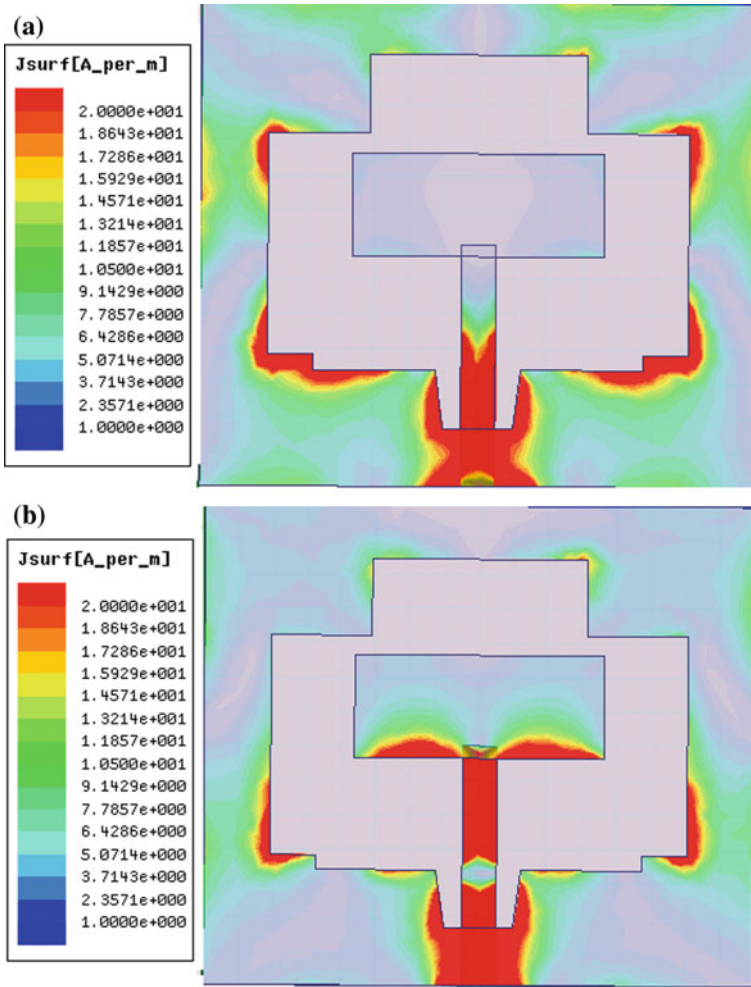


Fig. 23 a 9 GHz. b 10.4 GHz

Fig. 24 Gain Total in dB at 3.05 GHz

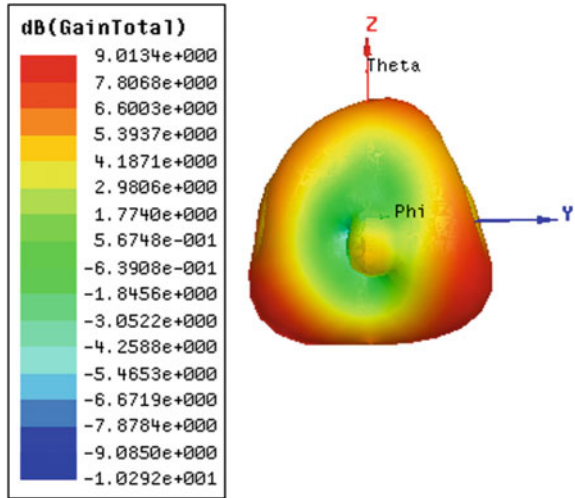


Fig. 25 Gain Total in dB at 4.1 GHz

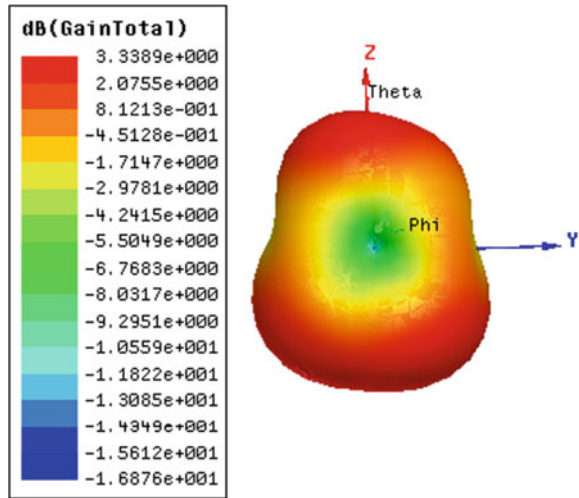


Fig. 26 Gain Total in dB for at 5.5 GHz

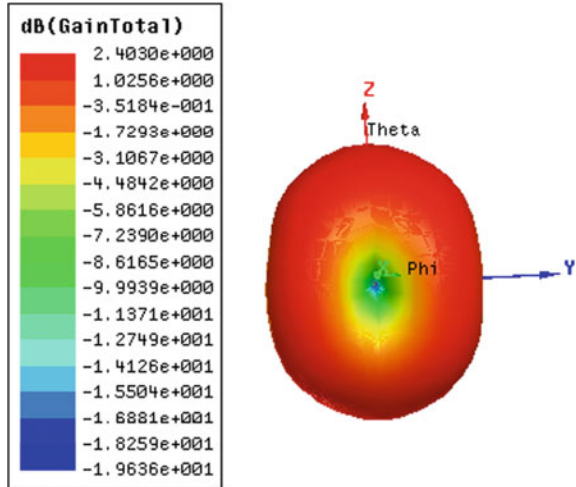


Fig. 27 Gain Total in dB at 7 GHz

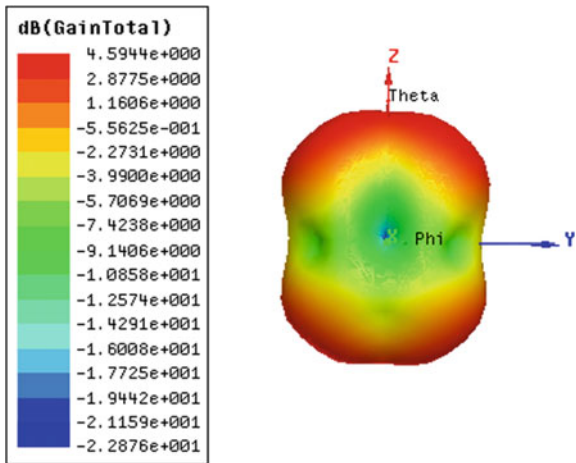


Fig. 28 Gain Total in dB at 8.3 GHz

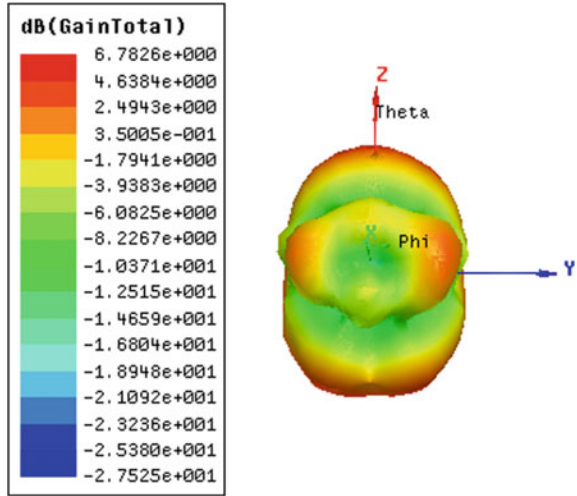


Fig. 29 Gain Total in dB at 9.28 GHz

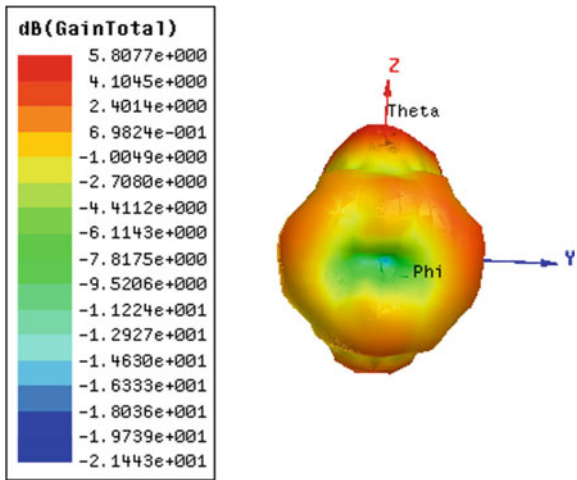
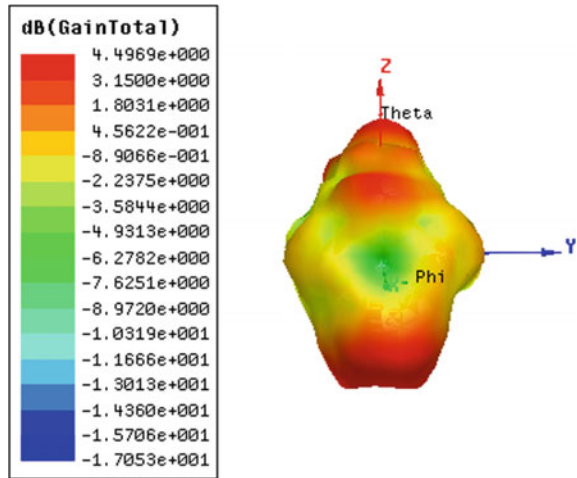


Fig. 30 Gain Total in dB at 10.4 GHz



4 Conclusion

A micro-strip feed slotted ground antenna was proposed and demonstrated in this study. According to the simulation results, the UWB band can be obtained by properly selecting the variable parameters of the antenna and optimizing the values. The return loss is below -10 dB for the whole band and the radiation pattern was monitored within the band and showed an acceptable omnidirectional pattern.

References

1. Ranga Y, Esselle KP, Weily AR (2010) Compact ultra-wideband CPW-fed printed semicircular slot antenna. *Microw Opt Technol Lett* 52(10):2367–2372
2. Liu WC (2005) Broadband dual-frequency cross-shaped slot CPW fed monopole antenna for WLAN operation. *Microw Opt Technol Lett* 46(4):353–355
3. Shagar AC, Wahidabanu RSD (2010) New design of CPW fed rectangular slot antenna for ultra wideband applications. *Int J Electron Eng* 2(1):69–73
4. Lin SY, Wong KL (2001) A dual-frequency micro-strip line fed printed slot antenna. *Microw Opt Technol Lett* 28:373–375
5. Morioka T, Araki S, Hirasawa K (1977) Slot antenna with parasitic element for dual band operation. *Electron Lett* 33:2093–2094
6. Li P, Liang J, Chen X (2006) Study of printed elliptical/circular slot antennas for ultra wide band applications. *Trans Antennas Propag* 54(6):1670–1675
7. Gand Ma T, Tseng CH (2006) An ultra wide band coplanar waveguide-fed tapered ring slot antenna. *IEEE Trans Antennas Propag* 54(4):1105–1110
8. Bostani A, Denidni TA (2008) Design of a new ultra wideband antenna with band rejection in WLAN frequencies. In: 2008 IEEE antennas and propagation society international symposium

9. Lee KF, Luk KM, Tong KF et al (1977) Experimental and simulation studies of the coaxially fed U-slot rectangular patch. *IEEE Proc Microw Antenna Propag* 144(5):354–358
10. Habib MA et al (2010) Ultra wideband CPW-fed aperture antenna with WLAN band rejection. *Progress Electromagn Res* 106:17–31
11. Bostani A, Webb JP (2011) A sparse finite-element method for modeling evanescent modes in the stopband of periodic structures. *IEEE Trans Magn* 47(5):1186–1189
12. Bostani A, Webb JP (2011) A model-order reduction method for the passband and stopband characteristics of periodic structures. In: 2011 41st European microwave conference, Manchester, pp 167–170